Talanta 232 (2021) 122415

Contents lists available at ScienceDirect

Talanta

journal homepage: www.elsevier.com/locate/talanta

Ultrasensitive detection of gene-PIK3CA^{H1047R} mutation based on cascaded strand displacement amplification and *trans*-cleavage ability of CRISPR/Cas12a

Yuanyi Deng [a,1], Gaihua Cao [a,1], Xiaolong Chen [a,1], Mei Yang [a], Danqun Huo [a,b,**], Changjun Hou [a,b,*]

[a] Key Laboratory for Biorheological Science and Technology of Ministry of Education, State and Local Joint Engineering Laboratory for Vascular Implants, Bioengineering College of Chongqing University, Chongqing, 400044, PR China

[b] Chongqing Key Laboratory of Bio-perception & Intelligent Information Processing, School of Microelectronics and Communication Engineering, Chongqing University, Chongqing, 400044, PR China

ARTICLE INFO

Keywords:
Gene-PIK3CA^{H1047R} mutation
Strand displacement amplification (SDA)
CRISPR/Cas12a
Fluorescent biosensor

ABSTRACT

Low abundance gene-PIK3CA^{H1047R} mutation detection is crucial for the clinical diagnosis and treatment of breast cancer. Here, a fluorescent biosensor which combines cascaded strand displacement amplification (C-SDA) and *trans*-cleavage ability of CRISPR/Cas12a was established to ultra-sensitively detect gene-PIK3CA^{H1047R} mutation. The mutated gene-PIK3CA^{H1047R} can combine with complementary sequence to form an intact recognition site for endonuclease FspI. Mediated by FspI, it breaks at the mutation site to produce DNA fragment to trigger SDA or C-SDA. Then, the fluorescent biosensors based on SDA-CRISPR/Cas12a or C-SDA-CRISPR/Cas12a were constructed. Compared with biosensor based on SDA-CRISPR/Cas12a (5 pM), the minimum detection of the biosensor based on C-SDA-CRISPR/Cas12a is reduced two orders of magnitude (50 fM). In range of 0.001%–50%, we achieved the ultrasensitive detection of gene-PIK3CA^{H1047R} mutation low to 0.001%. Besides, the proposed biosensor works well in human serum samples, showing its application potential in low-abundance gene-PIK3CA^{H1047R} mutation detection.

1. Introduction

Breast cancer is one of the predisposed cancers worldwide and the leading reason to cancer-related deaths in women. Nowadays, millions of people are diagnosed with breast cancer each year, which poses a serious threat to human life and health [1]. Early diagnosis and treatment of breast cancer can alleviate the suffering of patients and increase the cure rate greatly. Therefore, early diagnosis of breast cancer is urgently needed. Research found that PI3K pathway was activated in about 70% of breast cancer cases. In PI3K pathway, gene-PIK3CA^{H1047R} (phosphoinositide-3-kinase, catalytic alpha polypeptide), which encodes the catalytic α subunit of PI3K, is frequently mutated by internal and external factors, resulting in development of breast cancer [2]. Thus, the mutation of gene-PIK3CA^{H1047R} is potent predictive biomarker of the early-stage breast cancer [3]. Early discovery and detection of gene-PIK3CA^{H1047R} mutations will be of great significance for diagnosis, individualized therapy, and prognosis of breast cancer [4–7]. Furthermore, belongs to circulating tumor DNAs (ctDNAs) released by tumor cells, gene-PIK3CA^{H1047R} mutation can be detected by liquid biopsy [8]. Compared with traditional tissue biopsy, it can be sampled repeatedly and monitor the dynamic changes of the tumor accurately [9]. Regrettably, the concentration of gene-PIK3CA^{H1047R} mutation is low abundance under the high background of normal circulating DNAs [10]. So far, different methods for ctDNA have been reported, such as polymerase chain reaction (PCR) [11], DNA sequencing [12], colorimetry [13,14], electrochemistry [15,16], surface-enhanced Raman scattering (SERS)

* Corresponding author. Key Laboratory for Biorheological Science and Technology of Ministry of Education, State and Local Joint Engineering Laboratory for Vascular Implants, Bioengineering College of Chongqing University, Chongqing, 400044, PR China.

** Corresponding author. Chongqing Key Laboratory of Bio-perception & Intelligent Information Processing, School of Microelectronics and Communication Engineering, Chongqing University, Chongqing, 400044, PR China.

E-mail addresses: huodq@cqu.edu.cn (D. Huo), houcj@cqu.edu.cn (C. Hou).

[1] These authors contributed equally to this work.

https://doi.org/10.1016/j.talanta.2021.122415
Received 6 February 2021; Received in revised form 22 March 2021; Accepted 7 April 2021
Available online 20 April 2021

[17,18], and so on. Those sensing platforms own their advantages such as precise and sensitive, but they also have some disadvantages, such as time-consuming, cumbersome operation steps, and large instruments needed. For example, Li utilized doxorubicin@tetrahedron-Au (DOX@TDN-Au) as indicator and coupled it with rolling circle amplification (RCA) to establish an electrochemical biosensor. They used this method achieve the detection of ctDNA low to 0.29 fM [19]. Unfortunately, the complicated design of the DNA probe, tedious modification of electrode, and long analysis time limited the clinical application of this method. Due to ctDNAs are short-lived, easily degraded, and low abundance in body fluids. The sensitive and rapid detection of gene--PIK3CA^{H1047R} mutation is still of great significance for cancer prediction and individualized treatment.

Recently, different kinds of isothermal amplification methods have been proposed for sensitive detection of nucleic acids, such as exponential amplification reaction (EXPAR) [20], rolling circle amplification (RCA) [21], hybridization chain reaction (HCR) [22], strand displacement amplification (SDA) [23]. Among those, SDA shows an excellent versatility and amplification efficiency. Moreover, SDA is easy to design and simple to operate, and can be widely used in nucleic acid detection [24,25]. For instance, Xu combined SDA and target recycling amplification (TRA) to design a hairpin probe with a nicking site to develop a STAT3 sensing [26]. The established sensing platform showed good specificity and sensitivity in ctDNA detection. This shows that SDA has a good ability in nucleic acid detection and can improve the sensitivity of the sensor. But the use of SDA alone cannot meet the requirements of low-abundance ctDNA detection in blood.

CRISPR/Cas systems have been widely used in the field of gene editing. Among them, the Cas13, Cas12a, and Cas14 have indirect non-specific collateral cleave activity after specifically recognizing and cleave target single strand nucleic acid sequence indiscriminately. This characteristic can be utilized for nucleic acid detection, such as generating fluorescent signals by degrading labeled molecular beacons [27]. Bonini believed that PCR was indeed a revolution in gene analysis, but it requires a careful purification process, which is not easy to achieve in a point-of-care (POC) device. However, the latest new CRISPR/Cas strategies seem to offer unprecedented possibilities [28]. Wang also commented that recent reports on the use of CRISPR have shown their promise to redefine nucleic acid detection methods [29]. Biosensor based on CRISPR/Cas is widely considered as an innovative technology for the next-generation of diagnostics, which is gradually becoming mature with the efforts of researchers [30]. For example, Mukama introduced CRISPR/Cas12a system into lateral flow biosensor [31]. The reported approach employed CRISPR/Cas12 system and loop-mediated isothermal amplification to detect *Pseudomonas aeruginosa* acyltransferase gene, which could test the DNA target down to attomolar. Additionally, the combination of electrochemical sensing and CRISPR Cas9/Cas12a technology has also been reported. Without other enzymatic amplification method, the CRISPR/Cas system enhanced electrochemical DNA sensor exhibited femtomolar sensitivity [32]. Based on RT-PCR and CRISPR/Cas12a, Huang proposed a fluorescent strategy that could sensitively detect SARS-CoV-2 positive samples [33]. All above research indicated that the CRISPR/Cas system has great potential in nucleic acid detection.

PIK3CA^{H1047R} mutation is one of the common PIK3CA mutations in breast cancer. To develop a sensitive platform for PIK3CA^{H1047R} mutation detection, FspI is introduced to identify and cut targets to produce primers that trigger SDA or C-SDA. Here, we compared the amplification efficiency of SDA and C-SDA at the same target concentration firstly. Results found that the amplification efficiency of C-SDA was two orders of magnitude better than SDA. Based on C-SDA, large number of activators which can unlock the *trans*-cleavage activity of CRISPR/Cas12a were obtained. By coupling with the signal amplification function of the activated CRISPR/Cas12a system itself, this biosensor owns potential to realize ultrasensitive detection of gene-PIK3CA^{H1047R} mutation. The low abundance and complex detection environment of gene-PIK3CA^{H1047R} mutation make it difficult to detect gene-PIK3CA^{H1047R} mutation. But this biosensor is expected to solve this problem.

2. Experiment section

2.1. Reagents and equipment

Table S1 shows all DNA fragments used in the text, and they were all bought from Sangon Biotech (Shanghai, China). The synthesized crRNA was purified by MiRcute miRNA Isolation Kit (DP501) ordered from TIANGEN Biotechnology Co., Ltd (Beijing, China). The HiScribe T7 Quick High Yield RNA Synthesis Kit, T7 Mix, LbCas12a, 10 × NEB buffer 2.1, DNase I, FspI (10000 U/mL), 10 × CutSmart, Klenow Fragment (5000 U/mL), 10 × NEB buffer 2, and Nt.BbvCI (10000 U/mL) were offered by New England Biotechnology Co., Ltd (Beijing, China). The mixture of deoxy-ribonucleoside triphosphate (dNTPs) was provided by Sangon Biotech (Shanghai, China). Normal human serum was supplied by Solarbio Science & Technology Co., Ltd (Beijing, China). Fluorescence spectra of the final system were measured by LS-55 spectrofluorometer (P.E. USA). Parameters were set as follows: excitation and emission wavelength were set at 490 nm and 556 nm during the scan range from 400 nm to 700 nm. The corresponding slit widths were set at 12 nm and 10 nm, respectively.

2.2. Synthesis of crRNA

The crRNA of CRISPR/Cas12a was synthesized using T7 polymerase and the designed template. Specific steps of synthesis and purification can be seen in our previous work [34]. To ensure the stability of the in vitro transcription assay, three sets of replications were carried out. After measurement, its mean concentration was 725.7 ng/μL.

2.3. Amplification of activators though FspI-mediated strand displacement amplification (FspI-SDA) or FspI-mediated cascade strand displacement amplification (FspI-C-SDA)

First, 10 μL of mixture which contained 20 nM complementary sequence (CS), different concentrations of gene-PIK3CA^{H1047R} mutation fragment, 1 U FspI, and 1 × CutSmart buffer were incubated at 37 °C for 30 min. The gene-PIK3CA^{H1047R} mutation fragment and CS can form double stranded DNA which contains complete recognition site of FspI. Then, 1 μL of 200 nM template 1 or template 2, 1 U Klenow Fragment (KF), 1 U Nt.BbvCI, 1.5 μL 10 × CutSmart buffer, 2 μL 10 × NEB buffer 2, 1 μL of 10 mM dNTP were added. The final volume of the system was adjusted to 20 μL using ddH_2O. Finally, the mixture was mixed thoroughly and incubated at 37 °C for 60 min.

2.4. Measurement of the signal

Here, the activators generated by SDA or C-SDA were designed to include a 23 bp poly-T sequence. Correspondingly, the identifiable area of crRNA was designed to include 23 bp of poly-A sequence. Once the *trans*-cleavage activity of CRISPR/Cas12a was activated by the activators, the single-stranded DNA reporters will be cleaved indiscriminately and produce a fluorescent signal. Concretely, 4 μL of amplification products, 2 μL 10 × NEB buffer 2.1, 2 μL of 1 μM crRNA, 2 μL of 1 μM LbCas12a, 1 μL of 10 μM ssDNA reporters were mixed to a 20 μL reaction system and incubated at 37 °C for 40 min. Afterwards, 80 μL ddH_2O was added to stop the reaction and the obtained system was transferred to a fluorescent cuvette. The fluorescence signal of the system was detected at an excitation wavelength of 490 nm on a fluorometer.

2.5. Gel electrophoresis

The synthesis of crRNA was verified by 3% agarose electrophoresis. It was performed in 1 × TBE running buffer at 120 V for 50 min. A bright

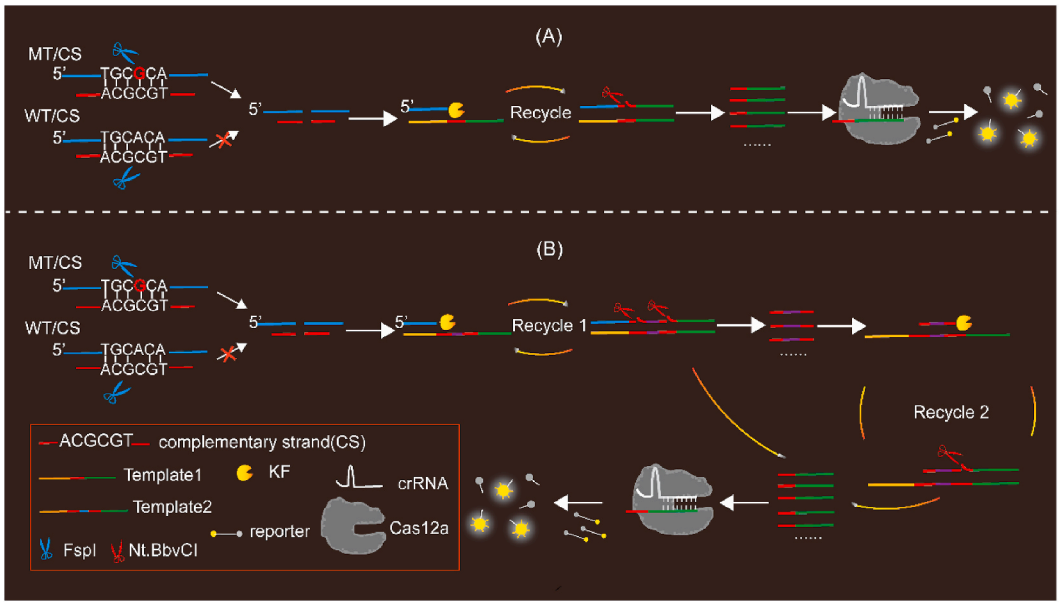

Scheme 1. Principle diagram of gene-PIK3CA^{H1047R} mutation detection based on SDA-CRISPR/Cas12a (A) or C-SDA-CRISPR/Cas12a (B).

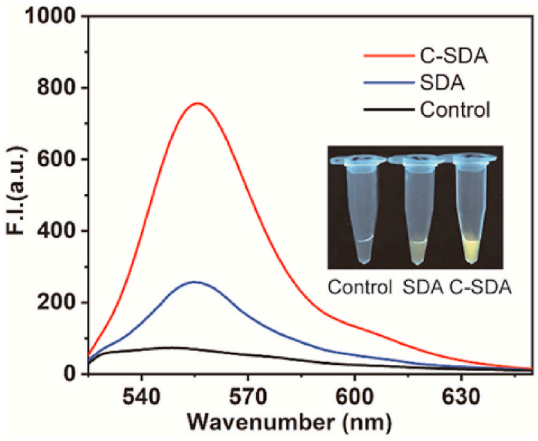

Fig. 1. Feasibility of the biosensor characterized by fluorescent signals based on SDA-CRISPR/Cas12a and C-SDA-CRISPR/Cas12a.

band is shown in Fig. S1, proving the successful synthesis of crRNA. Feasibility of SDA and C-SDA were confirmed by 15% of polyacrylamide gel electrophoresis (PAGE). The electrophoresis was executed in 1 × TBE buffer at 120 V for 60 min. Gel images were acquired by an Azure Biosystems C150 (USA).

3. Results and discussions

3.1. Principle of the gene-PIK3CA^{H1047R} mutation detection

The principle of gene-PIK3CA^{H1047R} mutation detection is illustrated in Scheme 1. Compared with the wild type gene-PIK3CA^{H1047R} (WT), the mutated gene-PIK3CA^{H1047R} (MT) contains the recognition sequence "-*TGC**G**CA*-" which can combine with complementary sequence (CS) to form an intact recognition site for endonuclease FspI. In the presence of FspI, gene-PIK3CA^{H1047R} mutation is cleaved at the mutation site, producing a DNA fragments that can trigger SDA or C-SDA. While the wild type gene-PIK3CA^{H1047R} can't be identified and cut by FspI due to the wild type gene-PIK3CA^{H1047R} can't form an intact recognition site for endonuclease FspI with CS. Here, we designed two different templates

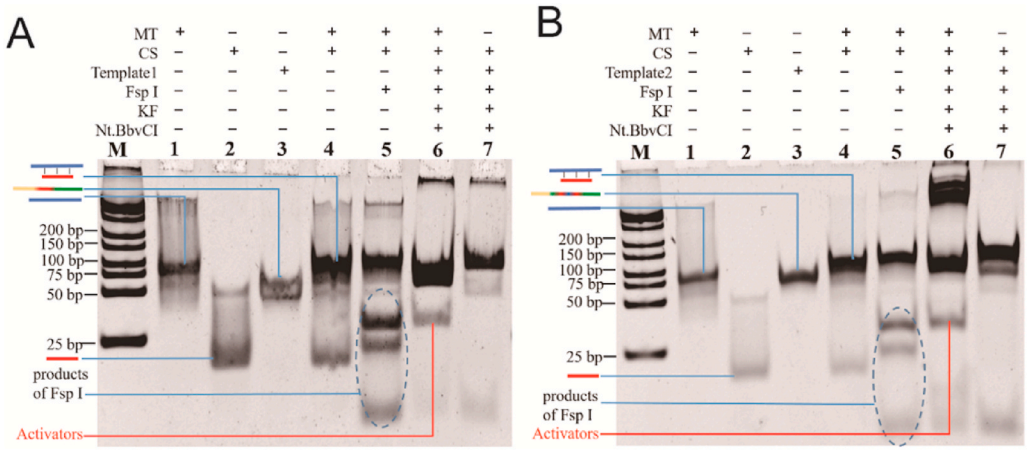

Fig. 2. Analysis of gel electrophoresis of SDA (A) and C-SDA (B). M: marker; Lane 1: gene-PIK3CA^{H1047R} mutation fragment; Lane 2: complementary sequence (CS); Lane 3: template 1 or template 2; Lane 4: the complex of gene-PIK3CA^{H1047R} mutation fragment and its complementary sequence; Lane 5: the mixture of complex digested by Fsp I; Lane 6: the experimental group; Lane 7: the control group.

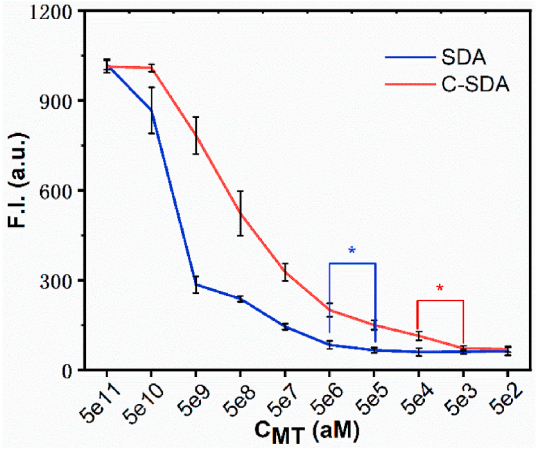

Fig. 3. Fluorescence response of biosensor based on SDA-CRISPR/Cas12a and C-SDA-CRISPR/Cas12a with different concentrations of gene-PIK3CA^{H1047R} mutation fragment (5×10^{11} to 5×10^{2} aM).

(template 1 and template 2). Compared with template 1, template 2 contains two endonuclease sites for Nt.BbvCI enzyme, so the generated intermediate chains can bind with the template 2 and act as primers to induce the next SDA (Scheme 1B). As a result, many activators which can unlock the *trans*-cleavage activity of CRISPR/Cas12a are obtained. Through the specific pairing between the activators and crRNAs, CRISPR/Cas12a's *trans*-cleavage activity is motivated. Once it is activated, the single-stranded DNA reporters that have modified with fluorophore and fluorescence quenching group at its ends can be cleaved indiscriminately, producing yellow fluorescence. Therefore, the fluorescence intensity of the system is positively correlated with the content of gene-PIK3CA^{H1047R} mutation.

3.2. Feasibility of the strategy

To inspect the feasibility of the developed biosensor, the detection of gene-PIK3CA^{H1047R} mutation based on SDA-CRISPR/Cas12a and C-SDA-CRISPR/Cas12a were done at the same target concentration (5 nM). As revealed in Fig. 1, the fluorescence signals of the test groups are significantly higher than the control group, indicating that the proposed biosensor owns an intense fluorescent response to the target. In addition, the fluorescence value of the test group based on the C-SDA-CRISPR/Cas12a is higher than the test group based on the SDA-CRISPR/Cas12a. This result illustrates that the C-SDA may have higher amplification efficiency to produces more activators under the same target concentration.

To prove that the activators are only produced in the existence of the target, we conducted a 15% polyacrylamide gel electrophoresis (PAGE) analysis. In Fig. 2A and B, the lines from left to right represent marker, gene-PIK3CA^{H1047R} mutation fragment, complementary sequence, template 1 or template 2, the complex of gene-PIK3CA^{H1047R} mutation fragment and its complementary sequence, the mixture of complex digested by FspI, the experimental group and the control group, respectively. In Lane 4, the band is higher than the gene-PIK3CA^{H1047R} mutation fragment (Lane 1) and the complementary sequence (Lane 2), implicating that partial DNAs have been combined into double-stranded DNA. In the presence of FspI, the dsDNA is cut at the restriction site to produce multiple bands, which includes the primer that can couple to the template 1 or template 2 to induce SDA or C-SDA (Lane 5). In Lane 6, the primers are combined with template 1 or template 2 to conduct cycle of polymerization, shearing, and substitution by KF and Nt.BbvCI, producing large number of activators. While in the control group (Lane 7), no corresponding band on behalf of activators are seen, indicating that FspI don't recognize and cut the double-stranded DNA formed by the wild-type gene-PIK3CA^{H1047R} and CS. These results indicate that the activators are only produced in the existence of the target.

3.3. Comparison of the strategy based on SDA-CRISPR/Cas12a or C-SDA-CRISPR/Cas12a

To verify that C-SDA is more efficient than SDA, we conducted further experimental exploration. As shown in Fig. 3, the fluorescence intensity of the biosensor based on SDA-CRISPR/Cas12a or C-SDA-CRISPR/Cas12a has been detected at different concentrations of targets. At the same target concentration, the fluorescence intensity of the biosensor based on the C-SDA-CRISPR/Cas12a is generally higher than the biosensor based on the SDA-CRISPR/Cas12a. For SDA, the fluorescence value increases slowly when the concentration of the gene-PIK3CA^{H1047R} mutation fragment increases from 500 aM to 500 pM, while the fluorescence value increases sharply when the gene-PIK3CA^{H1047R} mutation is greater than 500 pM. This is because SDA renders only one polymerization, cutting and replacement cycle to produce activators. Therefore, the biosensor based on SDA-CRISPR/Cas12a works not ideally in the low concentration of gene-PIK3CA^{H1047R} mutation fragment. In contrast, the fluorescence value of biosensor based on C-SDA-CRISPR/Cas12a rises steadily with the increase of the gene-PIK3CA^{H1047R} mutation fragment. C-SDA with two cycles gradually triggered by targets is responsible for this phenomenon, producing lots of activators to unlock the *trans*-cleavage of CRISPR/Cas12a. Compared with biosensor based on SDA-CRISPR/Cas12a (5 pM), the minimum corresponding concentration of biosensor based on C-SDA-CRISPR/Cas12a (50 fM) is two orders of magnitude lower.

3.4. Optimization of the biosensor based on C-SDA-CRISPR/Cas12a

To improve the performance of this biosensor, two pivotal experimental parameters: the reaction time of C-SDA and the cleavage time of the CRISPR/Cas12a were optimized. As exhibited in Fig. 4A, the value of $\triangle F$ ($\triangle F$=F–F', where F refers to the fluorescence value of the

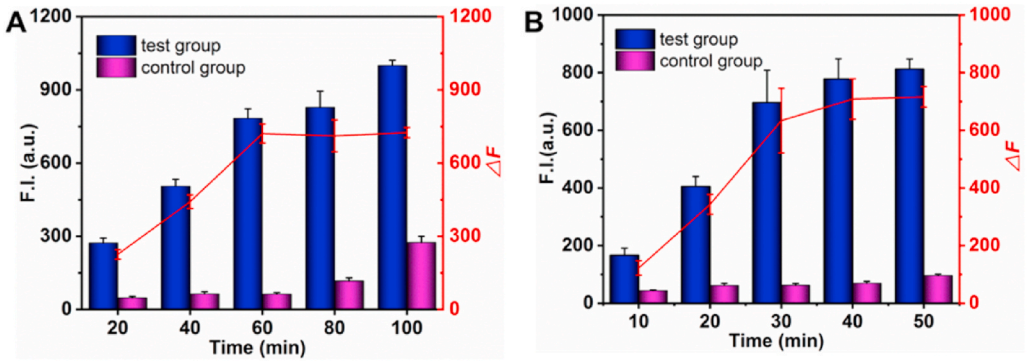

Fig. 4. Optimizations of the reaction time of C-SDA (A) and the cleavage time of CRISPR/Cas12a (B).

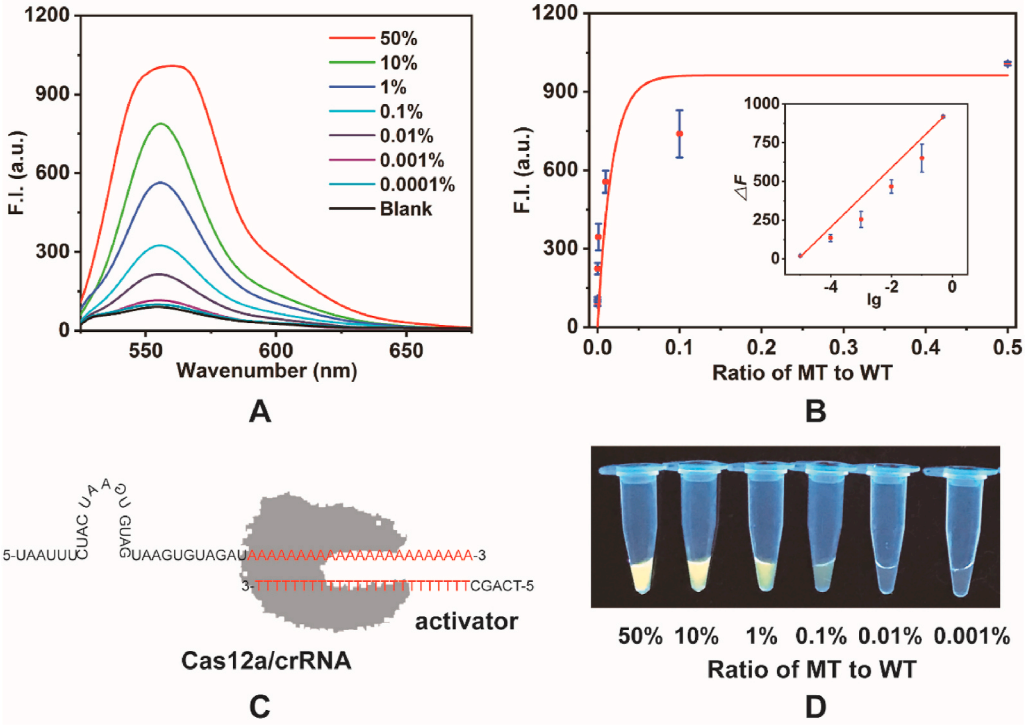

Fig. 5. Fluorescence spectrum (A) and corresponding fluorescence value (B) when the ratio of MT to WT is between 0% and 50% (Illustration shows the linear relationship between $\triangle F$ and the logarithmic value of the ratio in ranging of 0.001%–50%). Details drawing of activated CRISPR/Cas12a system (C) and the fluorescence shot (D) when the ratio of MT to WT is ranging of 0.001%–50%.

experimental group, F' refers to the fluorescence value of the control group) increases with the reaction time of C-SDA rises from 20 min to 60 min. From then on, the value of $\triangle F$ changes insignificantly. This may be because the nonspecific amplification emerges with the reaction time increases, resulting in a larger background signal. Therefore, 60 min is selected as the ideal reaction time of C-SDA. Subsequently, the cleavage time of the CRISPR/Cas12a was improved. As illustrated in Fig. 4B, the fluorescent signals increase with the cleavage time of the CRISPR/Cas12a until to 40 min. If the time continues to extend, the non-specific cleavage of Cas12a will increase, leading to a larger background signal. Thus, 40 min is adopted as the optimal cleavage time of the CRISPR/Cas12a.

3.5. Detection of the gene-PIK3CA^{H1047R} mutation based on C-SDA-CRISPR/Cas12a

To assess the detection performance of this biosensor in detecting low abundance gene-PIK3CA^{H1047R} mutation, the fluorescence intensity of the system was investigated in different ratio of mutational gene-PIK3CA^{H1047R} fragment (MT) to wild type gene-PIK3CA^{H1047R} fragment (WT) (MT/WT, from 0.0001% to 50%). The concentration of WT was fixed at 5 nM, and the ratio was adjusted by adding different amounts of MT. Under the optimal conditions, the fluorescent response is enhanced with the increase of MT ratio from 0 to 50% (Fig. 5A). When the ratio of MT to WT ranges in 0.001%–50%, there present an ideal linear relationship between the $\triangle F$ and the logarithmic value of the ratio, and the linear regression equation is $\triangle F = 972.29+191.86$lgR, ($R^2 = 0.9962$), where $\triangle F$ represents the net difference between the experimental group and the control group, R represents the logarithmic value of the ratio (Fig. 5B). The actual limit of detection (LOD) is 0.001%. Fig. 5C show the details of the activated CRISPR/Cas12a system. In the presence of the targets, C-SDA produces large number of activators. Here, the activator is designed to contain a 23 bp poly-T sequence and the recognition region of crRNA is designed to contain 23 bp poly-A sequence, which avoids the background interference caused by the matching of the interfering strand and crRNA well. Fig. 5D displays the fluorescence shot when the ratio of MT to WT is ranging of 0.001%–50%. The fluorescence intensity of the system becomes darker as the ratio of MT to WT decreases. As the ratio of MT to WT decreases, the concentration of the target (MT) also decreases. Therefore, subsequent cleavage and amplification processes triggered by the target will also be reduced, resulting in a decrease in the final fluorescence intensity. Moreover, due to the excellent signal amplification of C-SDA and CRISPR/Cas12a, the proposed biosensor possesses significant advantages in sensitivity, which is superior to other reported biosensors (Table 1).

Table 1
Comparison with other reported biosensors for single-nucleotide variants detection.

Method	Platform	LOD	Time	Ref.
LCR and gold nanoparticle	Colorimetry	0.01%	>90 min	[35]
Strand displacement and selective digestion	Fluorescence	0.2%	>120 min	[36]
Controllable extension of hairpin-structured flaps	Fluorescence	0.02%	>200 min	[37]
Ligase-assisted, LRET-based method	Fluorescence	0.1%	>4 h	[38]
mismatched ligation-triggered cascade SDA	Colorimetry	0.2%	~4 h	[13]
Cationic conjugated polymers	Fluorescence	2%	>7 h	[39]
FspI based M-SDA-CRISPR/12a	Fluorescence	0.001%	~140 min	**This work**

3.6. Anti-interference ability of the biosensor based on C-SDA-CRISPR/Cas12a

To verify the anti-interference ability of the biosensor, several interfering DNA strands were selected for anti-interference experiments at the same concentration. The concentration of interfering DNA strands

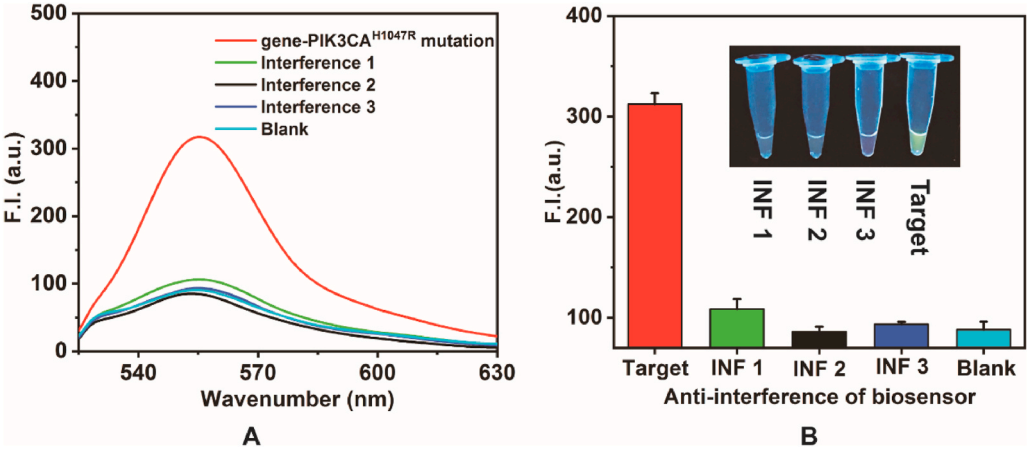

Fig. 6. Anti-interference ability of strategy. (A) fluorescence spectra and corresponding fluorescence values (B) of experimental group, interference groups and blank group.

Table 2
The proposed biosensor for gene-PIK3CA^{H1047R} mutation fragment detection in human serum samples.

Target added (%)	Detected results (%)	Recovery (%)
0	0.000911	–
0.01	0.00913	90.7
1	1.00383	100.3
10	11.4429	114.4

and target DNA strands were adjusted to 5 pM uniformly. Their fluorescence spectra (Fig. 6A) and corresponding fluorescence values were analyzed. Fig. 6B demonstrates that the fluorescence value of the experimental group is significantly higher than that of other interference groups and blank group, indicating that the proposed biosensor owns excellent anti-interference ability.

3.7. Detection of spiked samples in human serum samples

To study the practical application of the proposed biosensor based on C-SDA-CRISPR/Cas12a in actual samples, we utilized it to detect spiked ratio of MT to WT (10%, 1%, and 0.01%) in the human serum samples. Before use, it was diluted to 20 times though enzyme-free water. As shown in Table 2, the fluorescence intensity of the blank group also increases slightly, which may be caused by some non-specific interference or very small amount of mutated gene-PIK3CA^{H1047R} existed in the complex matrix. According to Table 2, the recovery rates of spiked samples are in the range of 90.7%–114.4%, indicating that the biosensor can be potentially used to detect gene-PIK3CA^{H1047R} mutation fragment in actual sample.

4. Conclusions

In summary, an ultrasensitive biosensor which couples C-SDA and the *trans*-cleavage activity of CRISPR/Cas12a was established to detect gene-PIK3CA^{H1047R} mutation fragment. We cleverly took advantage of the mutated gene-PIK3CA^{H1047R} with the recognition site of endonuclease FSpI to identify and handle the target. The combination of gene-PIK3CA^{H1047R} mutation fragment and complementary sequence is cleaved into multiple small DNA fragments in the presence of FSpI. Combining with the high-efficiency amplification of C-SDA and the amplification function of the CRISPR/Cas12a, this biosensor achieves the ultrasensitive detection of gene-PIK3CA^{H1047R} mutation. Besides, this biosensor possesses excellent anti-interference ability and performs well in the analysis of gene-PIK3CA^{H1047R} mutation in human serum samples. The low abundance of gene-PIK3CA^{H1047R} mutation makes it difficult to detect it. While the proposed biosensor is hoped to solve this problem due to its property with highly sensitive, easy to operate, and time-saving.

Author statement outlining

Yuanyi Deng: Conceptualization, Methodology, Roles/Writing - original draft. Gaihua Cao: Validation, Methodology and Formal analysis. Xiaolong Chen: Conceptualization, Methodology, Writing - Original Draft, Writing - Review & Editing. Mei Yang: Methodology, Software. Danqun Huo: Supervision, Project administration. Changjun Hou: Writing - Review & Editing, Project administration, Funding acquisition.

Declaration of competing interest

The authors declare that they have no known competing financial interests or personal relationships that could have appeared to influence the work reported in this paper.

Acknowledgment

This work was supported by the National Natural Science Foundation of China (81772290 and 81271930), Graduate Scientific Research and Innovation Foundation of Chongqing, China (CYS20076 and CYB20070), Fundamental Research Funds for the Central Universities (2019CDYGZD007) , The Higher Education Teaching Reform Research Project of Chongqing (203249), Chongqing Graduate Tutor Team Construction Project, Analytical and Testing Center of Chongqing University and the sharing fund of Chongqing University's large equipment.

Appendix A. Supplementary data

Supplementary data to this article can be found online at https://doi.org/10.1016/j.talanta.2021.122415.

References

[1] J. Ferlay, M. Colombet, I. Soerjomataram, C. Mathers, D.M. Parkin, M. Pineros, A. Znaor, F. Bray, Estimating the global cancer incidence and mortality in 2018: GLOBOCAN sources and methods, Int. J. Canc. 144 (8) (2019) 1941–1953, https://doi.org/10.1002/ijc.31937.

[2] T. Shimoi, A. Hamada, M. Yamagishi, M. Hirai, M. Yoshida, T. Nishikawa, K. Sudo, A. Shimomura, E. Noguchi, M. Yunokawa, K. Yonemori, C. Shimizu, T. Kinoshita, T. Fukuda, Y. Fujiwara, K. Tamura, PIK3CA mutation profiling in patients with breast cancer, using a highly sensitive detection system, Canc. Sci. 109 (8) (2018) 2558–2566, https://doi.org/10.1111/cas.13696.

[3] Y. Huang, M. Tao, S. Luo, Y. Zhang, B. Situ, X. Ye, P. Chen, X. Jiang, Q. Wang, L. Zheng, A novel nest hybridization chain reaction based electrochemical assay for sensitive detection of circulating tumor DNA, Anal. Chim. Acta 1107 (2020) 40–47, https://doi.org/10.1016/j.aca.2020.02.006.
[4] T. Yoshinami, N. Kagara, D. Motooka, S. Nakamura, T. Miyake, T. Tanei, Y. Naoi, M. Shimoda, K. Shimazu, S.J. Kim, S. Noguchi, Detection of ctDNA with personalized molecular barcode NGS and its clinical significance in patients with early breast cancer, Transl Oncol 13 (8) (2020) 100787, https://doi.org/10.1016/j.tranon.2020.100787.
[5] E. Tzanikou, A. Markou, E. Politaki, A. Koutsopoulos, A. Psyrri, D. Mavroudis, V. Georgoulias, E. Lianidou, PIK3CA hotspot mutations in circulating tumor cells and paired circulating tumor DNA in breast cancer: a direct comparison study, Mol Oncol 13 (12) (2019) 2515–2530, https://doi.org/10.1002/1878-0261.12540.
[6] C. Gasch, T. Oldopp, O. Mauermann, T.M. Gorges, A. Andreas, C. Coith, V. Muller, T. Fehm, W. Janni, K. Pantel, S. Riethdorf, Frequent detection of PIK3CA mutations in single circulating tumor cells of patients suffering from HER2-negative metastatic breast cancer, Mol Oncol 10 (8) (2016) 1330–1343, https://doi.org/10.1016//j.molonc.2016.07.005.
[7] A. Ferreira-Gonzalez, Plasma PIK3CA mutation testing in advanced breast cancer patients for personalized medicine: a value proposition, J Appl Lab Med 5 (5) (2020) 1076–1089, https://doi.org/10.1093/jalm/jfaa117.
[8] M. Elazezy, S.A. Joosse, Techniques of using circulating tumor DNA as a liquid biopsy component in cancer management, Comput. Struct. Biotechnol. J. 16 (2018) 370–378, https://doi.org/10.1016/j.csbj.2018.10.002.
[9] L. Gorgannezhad, M. Umer, M.N. Islam, N.T. Nguyen, M.J.A. Shiddiky, Circulating tumor DNA and liquid biopsy: opportunities, challenges, and recent advances in detection technologies, Lab Chip 18 (8) (2018) 1174–1196, https://doi.org/10.1039/C8LC00100F.
[10] X. Yi, J. Ma, Y. Guan, R. Chen, L. Yang, X. Xia, The feasibility of using mutation detection in ctDNA to assess tumor dynamics, Int. J. Canc. 140 (12) (2017) 2642–2647, https://doi.org/10.1002/ijc.30620.
[11] M.N. Emaus, J.L. Anderson, Allelic discrimination between circulating tumor DNA fragments enabled by a multiplex-qPCR assay containing DNA-enriched magnetic ionic liquids, Anal. Chim. Acta 1124 (2020) 184–193, https://doi.org/10.1016/j.aca.2020.04.078.
[12] Z. Cai, Z. Wang, C. Liu, D. Shi, D. Li, M. Zheng, H. Han-Zhang, A. Lizaso, J. Xiang, J. Lv, W. Wu, Z. Zhang, Z. Zhang, F. Yuan, S. He, J. Sun, Detection of microsatellite instability from circulating tumor DNA by targeted deep sequencing, J. Mol. Diagn. 22 (7) (2020) 860–870, https://doi.org/10.1016/j.jmoldx.2020.04.210.
[13] C. Shen, B. Shen, F. Mo, X. Zhou, X. Duan, X. Wei, J. Li, Y. Duan, W. Cheng, S. Ding, High-sensitive colorimetric biosensing of PIK3CA gene mutation based on mismatched ligation-triggered cascade strand displacement amplification, Sensor. Actuator. B Chem. 273 (2018) 377–383, https://doi.org/10.1016/j.snb.2018.06.041.
[14] X. Mao, S. Pan, D. Zhou, X. He, Y. Zhang, Fabrication of DNAzyme-functionalized hydrogel and its application for visible detection of circulating tumor DNA, Sensor. Actuator. B Chem. 285 (2019) 385–390, https://doi.org/10.1016/j.snb.2019.01.076.
[15] W. Ma, H. Du, M. Zhang, J. Mori, X. Ren, H. Wang, X. Zhang, One-step synthesis of tunable zinc-based nanohybrids as an ultrasensitive DNA signal amplification platform, ACS Appl. Mater. Interfaces 12 (2) (2020) 2983–2990, https://doi.org/10.1021/acsami.9b18973.
[16] H.F. Wang, R.N. Ma, F. Sun, L.P. Jia, W. Zhang, L. Shang, Q.W. Xue, W.L. Jia, H. S. Wang, A versatile label-free electrochemical biosensor for circulating tumor DNA based on dual enzyme assisted multiple amplification strategy, Biosens. Bioelectron. 122 (2018) 224–230, https://doi.org/10.1016/j.bios.2018.09.028.
[17] J. Zhang, Y. Dong, W. Zhu, D. Xie, Y. Zhao, D. Yang, M. Li, Ultrasensitive detection of circulating tumor DNA of lung cancer via an enzymatically amplified SERS-based frequency shift assay, ACS Appl. Mater. Interfaces 11 (20) (2019) 18145–18152, https://doi.org/10.1021/acsami.9b02953.
[18] Q. Zhou, J. Zheng, Z. Qing, M. Zheng, J. Yang, S. Yang, L. Ying, R. Yang, Detection of circulating tumor DNA in human blood via DNA-mediated surface-enhanced Raman spectroscopy of single-walled carbon nanotubes, Anal. Chem. 88 (9) (2016) 4759–4765, https://doi.org/10.1021/acs.analchem.6b00108.
[19] D. Li, Y. Xu, L. Fan, B. Shen, X. Ding, R. Yuan, X. Li, W. Chen, Target-driven rolling walker based electrochemical biosensor for ultrasensitive detection of circulating tumor DNA using doxorubicin@tetrahedron-Au tags, Biosens. Bioelectron. 148 (2020) 111826, https://doi.org/10.1016/j.bios.2019.111826.
[20] Y. Sun, Y. Sun, W. Tian, C. Liu, K. Gao, Z. Li, A novel restriction endonuclease GlaI for rapid and highly sensitive detection of DNA methylation coupled with isothermal exponential amplification reaction, Chem. Sci. 9 (5) (2018) 1344–1351, https://doi.org/10.1039/c7sc04975g.
[21] D. Li, T. Zhang, F. Yang, R. Yuan, Y. Xiang, Efficient and exponential rolling circle amplification molecular network leads to ultrasensitive and label-free detection of MicroRNA, Anal. Chem. 92 (2) (2020) 2074–2079, https://doi.org/10.1021/acs.analchem.9b04585.
[22] Q. Guo, Y. Yu, H. Zhang, C. Cai, Q. Shen, Electrochemical sensing of exosomal MicroRNA based on hybridization chain reaction signal amplification with reduced false-positive signals, Anal. Chem. 92 (7) (2020) 5302–5310, https://doi.org/10.1021/acs.analchem.9b05849.
[23] Z. Wu, F. Luo, W. Wen, X. Zhang, S. Wang, Enrichment-stowage-cycle strategy for ultrasensitive electrochemiluminescent detection of HIV-DNA with wide dynamic range, Anal. Chem. 91 (19) (2019) 12238–12245, https://doi.org/10.1021/acs.analchem.9b01969.
[24] A. Chen, G.F. Gui, Y. Zhuo, Y.Q. Chai, Y. Xiang, R. Yuan, Signal-off electrochemiluminescence biosensor based on Phi29 DNA polymerase mediated strand displacement amplification for MicroRNA detection, Anal. Chem. 87 (12) (2015) 6328–6334, https://doi.org/10.1021/acs.analchem.5b01168.
[25] M. Jiao, G. Jie, L. Tan, S. Niu, AgNPs-3D nanostructure enhanced electrochemiluminescence of CdSe quantum dot coupled with strand displacement amplification for sensitive biosensing of DNA, Anal. Chim. Acta 983 (2017) 166–172, https://doi.org/10.1016/j.aca.2017.06.022.
[26] H. Xu, B. Wu, J. Wang, H. Cao, J. Yang, K. Hao, S. Chen, S. Ye, Z. Shen, Label-free detection of cancer related gene based on target recycling and palindrome-mediated strand displacement amplification, Talanta 215 (2020) 120897, https://doi.org/10.1016/j.talanta.2020.120897.
[27] R. Aman, A. Mahas, M. Mahfouz, Nucleic acid detection using CRISPR/cas biosensing technologies, ACS Synth. Biol. 9 (6) (2020) 1226–1233, https://doi.org/10.1021/acssynbio.9b00507.
[28] A. Bonini, N. Poma, F. Vivaldi, A. Kirchhain, P. Salvo, D. Bottai, A. Tavanti, F. Di Francesco, Advances in biosensing: the CRISPR/Cas system as a new powerful tool for the detection of nucleic acids, J. Pharmaceut. Biomed. Anal. 192 (2021) 113645, https://doi.org/10.1016/j.jpba.2020.113645.
[29] M. Wang, R. Zhang, J. Li, CRISPR/cas systems redefine nucleic acid detection: principles and methods, Biosens. Bioelectron. 165 (2020) 112430, https://doi.org/10.1016/j.bios.2020.112430.
[30] Y. Li, S. Li, J. Wang, G. Liu, CRISPR/Cas systems towards next-generation biosensing, Trends Biotechnol. 37 (7) (2019) 730–743, https://doi.org/10.1016/j.tibtech.2018.12.005.
[31] O. Mukama, J. Wu, Z. Li, Q. Liang, Z. Yi, X. Lu, Y. Liu, Y. Liu, M. Hussain, G. G. Makafe, J. Liu, N. Xu, L. Zeng, An ultrasensitive and specific point-of-care CRISPR/Cas12 based lateral flow biosensor for the rapid detection of nucleic acids, Biosens. Bioelectron. 159 (2020) 112143, https://doi.org/10.1016/j.bios.2020.112143.
[32] W. Xu, T. Jin, Y. Dai, C.C. Liu, Surpassing the detection limit and accuracy of the electrochemical DNA sensor through the application of CRISPR Cas systems, Biosens. Bioelectron. 155 (2020) 112100, https://doi.org/10.1016/j.bios.2020.112100.
[33] Z. Huang, D. Tian, Y. Liu, Z. Lin, C.J. Lyon, W. Lai, D. Fusco, A. Drouin, X. Yin, T. Hu, B. Ning, Ultra-sensitive and high-throughput CRISPR-p owered COVID-19 diagnosis, Biosens. Bioelectron. 164 (2020) 112316, https://doi.org/10.1016/j.bios.2020.112316.
[34] X. Chen, G. Cao, X. Wang, Z. Ji, F. Xu, D. Huo, X. Luo, C. Hou, Terminal deoxynucleotidyl transferase induced activators to unlock the trans-cleavage of CRISPR/Cpf 1 (TdT-IU- CRISPR/Cpf 1): an ultrasensitive biosensor for Dam MTase activity detection, Biosens. Bioelectron. 163 (2020) 112271, https://doi.org/10.1016/j.bios.2020.112271.
[35] W. Shen, H. Deng, Z. Gao, Gold nanoparticle-enabled real-time ligation chain reaction for ultrasensitive detection of DNA, J. Am. Chem. Soc. 134 (36) (2012) 14678–14681, https://doi.org/10.1021/ja306265n.
[36] Y. Yu, T. Wu, A. Johnson-Buck, L. Li, X. Su, A two-layer assay for single-nucleotide variants utilizing strand displacement and selective digestion, Biosens. Bioelectron. 82 (2016) 248–254, https://doi.org/10.1016/j.bios.2016.03.070.
[37] Y.L. Liu, H.P. Wu, Q. Zhou, Q.X. Song, J.Z. Rui, X.X. Guan, G.H. Zhou, B.J. Zou, Controllable extension of hairpin-structured flaps to allow low-background cascade invasive reaction for a sensitive DNA logic sensor for mutation detection, Chem. Sci. 9 (6) (2018) 1666–1673, https://doi.org/10.1039/c7sc04210h.
[38] P. Wang, P. Zhang, Ligase-assisted, upconversion luminescence resonance energy transfer-based method for specific and sensitive detection of V600E mutation in the BRAF gene, RSC Adv. 4 (99) (2014) 56235–56240, https://doi.org/10.1039/c4ra10181b.
[39] B. Xing, J. Song, S. Ge, Z. Tang, M. Liu, Q. Yang, F. Lü, L. Liu, S. Wang, Multiplex detection of KRAS and BRAF mutations using cationic conjugated polymers, Chin. Sci. Bull. 58 (8) (2012) 873–878, https://doi.org/10.1007/s11434-012-5553-9.